Measurement of inverted n-hexane fireball properties with a Multipole Resonance Probe

G. Eichenhofer[1,6], M. Oberberg[2,3], P. Awakowicz[2], J. Eisenlohr[4] and J. Gruenwald[5,6]

[1] *4A-Plasma, Aichtalstraße 66, 71088 Holzgerlingen, Germany*
[2] *Institute of Electrical Engineering and Plasma Technology, University of Bochum, Universitätsstraße 150, 44801 Bochum, Germany*
[3] *House of Plasma GmbH, Universitätsstraße 136, 44799 Bochum, Germany*
[4] *Plasma Technology GmbH, Marie-Curie-Straße 8, 71083 Herrenberg-Gültstein, Germany*
[5] *Gruenwald Laboratories GmbH, Taxberg 50, 5660 Taxenbach , Austria*
[6] *Members of the GET-Plasma project consortium*

(Received: 18. Jan. 2022, Accepted: 31. Jan. 2022, Published online: 02. Feb. 2022)

In this paper we present for the first time the measurement of inverted fireballs in a low-pressure Ar/n-hexane plasma by using a Multipole Resonance Probe. The basic plasma parameters such as electron density, electron temperature and Debye length as well as the particle collision frequency have been obtained for different experimental settings. These measurements show that inverted fireballs that are created in chemically active plasma offer advantageous properties regarding deposition techniques. Furthermore, the influence of the plasma parameters on grid bias and changes in neutral gas pressure has been studied within this work. It is observed that the plasma density within an inverted fireball configuration can be raised by more than an order of magnitude compared to the background plasma or without biasing the grid electrode, respectively. The obtained results are promising for future coating and surface modification applications with inverted fireballs and show that the Multipole Resonance Probe is a viable diagnostic tool for reactive plasmas.

(DOI: 10.31281/jtsp.v3i1.23)

jgruenwald@g-labs.eu

I. Introduction

Since the first works on inverted fireballs (IFBs) were published in 2011 [1, 2] several papers focussing on instabilities and basic plasma parameters in IFBs followed [3-9]. However, since 2014 a number of works have been devoted to the application of IFBs in PECVD deposition processes [10-13]. Their unique properties in terms of elevated plasma density and homogeneity make them interesting candidates for future coating technologies. The most promising thin films obtained with IFBs are carbon containing coatings such as diamond like carbon (DLC), carbon nano walls and graphene. However, investigations on IFBs are still scarce, especially when it comes to their utilisation in coating processes or other surface modification applications. This article aims at broadening the understanding of the basic plasma properties of IFBs in low pressure reactive plasmas. The measurements conducted for this paper applied a Multipole Resonance Probe (MRP), which was developed at the Ruhr University Bochum. The recently developed MRP was modeled, simulated, experimentally validated and is described in various publications, e.g. Refs. [14-19]. The probe's principle is based on active plasma resonance spectroscopy with the measurement of the admittance of the plasma-probe-system [15, 16]. It uses the electron's ability to resonate at a frequency close to the electron plasma frequency. This resonance can be determined by the measurement technique. The probe head itself consists of two conducting hemispheres

(radius 3 mm), which are surrounded by a glass tube (thickness 1 mm) and separated by a dielectric low-temperature co-fired ceramic layer [18]. By coupling a low power (0.1 mW) sweeping rf signal from MHz to several GHz into the plasma and measuring the reflection coefficient with a vector network analyser the admittance's resonance frequency f_{res} as well as the signal's damping (full width at half maximum – FWHM) can be determined. It has to be noted, though, that the damping consists mainly of two contributions: one from actual collisions between the particles in the plasma and a second one from kinetic effects. The latter arise from electrons gaining and transporting the signal's energy by entering and leaving the region of the probe's influence. This leads to a collision less damping of the probe signal and has to be taken into account when analysing the data. From the frequency response the electron density n_e, electron collision frequency ν and an approximation for the electron temperature T_e of an assumed Maxwellian energy distribution function can be obtained [14, 15, 17]:

$\omega^2 \sim n_e$

$FWHM \sim \nu, T_e$

The probe measurements were conducted with a horizontally movable MRP, provided by House of Plasma from Ruhr University Bochum. The probe is connected to a PC with a user interface, a network analyser and an electronic control system. The probe itself was mounted on the vacuum chamber on one side and a small hole was cut into the IFB cage through which the MRP could enter the hollow anode and perform spatial scans. The advantage of using an MRP in reactive plasma is that coating of the surface is not a problem like it would be for Langmuir probes.

The paper is organised as follows: A description of the experimental setup, a presentation of the measured data and a discussion of the results.

II. Experimental Setup

All experiments in this work were carried out in a stainless steel vacuum chamber (Plasma Technology GmbH, PA 100) at different pressures, ranging from 1 to 6 Pa. The IFB grid anode was manufactured from a nickel plated stainless steel mess, which formed a prism with a height of 8.5 cm and an edge length of 18.5 cm. The grid constant was 250 µm and the mesh wires had a diameter of 120 µm. The chamber was connected to a turbo pump. The gas mixture used in the experiments consisted of Ar and n-hexane with a flow rate of 100 sccm each. The background plasma was created with a BeamTec DC 275V plasma generator from EDF Electronics, which was operated with a constant output power of 50 W. The probe measurements were conducted with a horizontally movable MRP, provided by the House of Plasma at the University of Bochum. The probe is connected to a PC with a user interface, a network analyser and an electronic control system. The probe itself was mounted on the vacuum chamber on one side and a small hole was cut into the IFB cage through which the MRP could enter the hollow anode and perform spatial scans. A picture of the probe and the IFB setup is shown in the following Fig. 1:

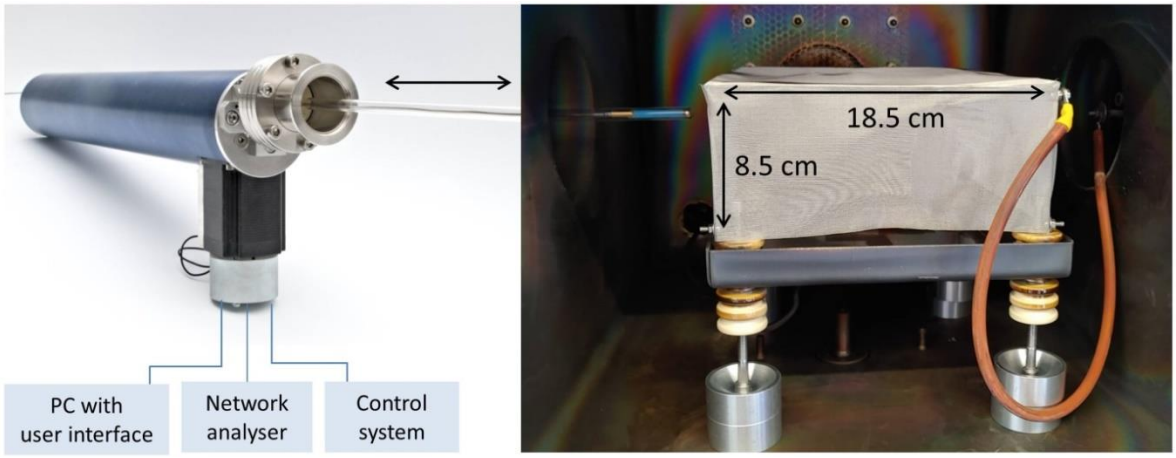

Figure 1: The plasma resonance probe provided by House of Plasma (University of Bochum) with schematic of the whole measurement system (left) and the IFB cage electrode inside the vacuum chamber (right).

The IFB cage was insulated from the rest of the chamber with a dielectric mount and was variably biased for different experiments. The floor plate of the IFB setup was also used to couple the power from the primary plasma source into the chamber. Two types of measurements were performed, radial scans starting at the centre point of the grid electrode up to about 2 cm away from the mesh cage. The measurements were stopped there to avoid distortions from the edges of the IFB, since it was observed in former experiments [8] that probe measurements can become somewhat disturbed when the probe is approaching the IFB edge. As a result the electron density and temperature profiles as well as the particle collision frequency were obtained. Further measurements in the centre plasma were performed at varying pressure and grid voltage. The results of these experiments are depicted in the next section.

III. Results

The first parameters that were measured were the radial profiles of the electron density n_e as shown in Fig. 2:

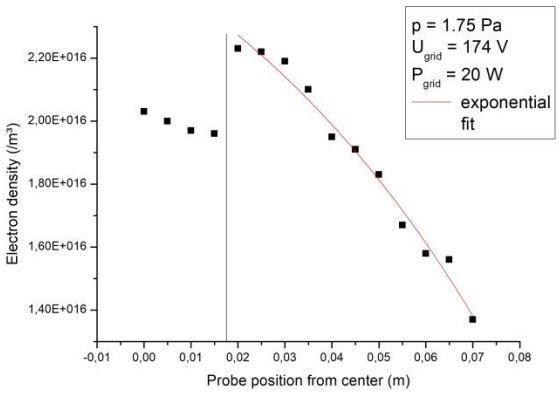

Figure 2: Radial profile of the electron density measured through the grid electrode. Experimental parameters: p = 1.75 Pa, U_{grid} = 174 V (at 20 W).

As can be seen in Fig. 2 the major part of n_e follows an exponential decay towards the edge of the IFB. This is to be expected as this is the usual behaviour of the charge density in IFBs [3, 8, 9]. However, there is a distinct jump in the density close to the centre of the fireball plasma. However, a measurement error can be ruled out because the electron temperature (T_e) profile shows no distinct jump at the position 1.5 cm away from the centre. However, if the electron density drops the electron temperature is expected to increase due to current continuity, which can as well explain the rise in Te, depicted in the following Fig. 3:

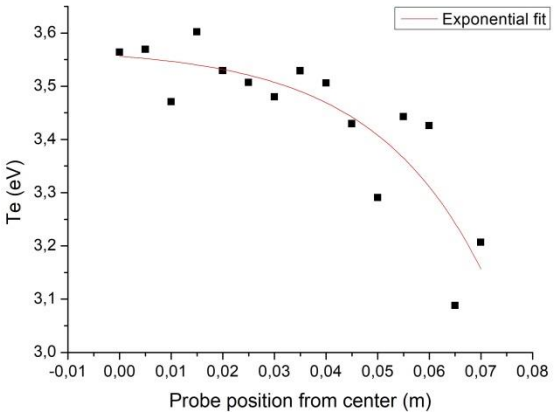

Figure 3: Radial profile of the electron temperature measured through the grid electrode. Experimental parameters: p = 1.75 Pa, U_{grid} = 174 V (at 20 W).

T_e follows a steady increase from around 3 eV near the edge of the IFB and saturates at around 3.6 eV at the centre. A reasonable explanation is that electrons attach themselves to fragments of the dissociated n-hexane molecules. Since the dissociation energy of these molecules is about 4.4 eV at room temperature [20] this process will most efficiently occur near the IFB centre where T_e is highest. It is also known that in the gas phase the most likely fractions of the n-hexane particles are C_2H and CH_3 radicals [21]. Especially the methyl radical can form anions with the highest formation yields at electron energies of 6.6 eV [22], which weakly binds electrons, diminishing the electron density in this volume by about 10 %. From this position on towards the centre of the discharge the electron density is again increasing exponentially because the remaining, unbound electrons with high enough energy start to ionise and dissociate the hydrocarbons via inelastic collisions. This is possible due to the total cross section for collisions between electrons and n-hexane particles, which is about 4 x 10^{-19} m² for 3 eV electrons [23]. Inserting this into the equation for the collision mean free path $\lambda=kT/(\sigma p)$, where k is Boltzmann's constant, T is the absolute temperature of the neutral gas (~300 to 350 K), σ is the cross section and p is the pressure in Pa, yields about 1 cm mean free path. This explanation fits to the measured data quite reasonable. However, it has to be noticed that the chemistry in hydrocarbon plasma is very complicated and a more detailed analysis of the dissociation process and the capture of slow electrons by the fragments is well beyond the scope of the work and, thus, left for future work.

From the measurements of n_e and T_e the Debye length λ_D was calculated and is depicted in Fig. 4:

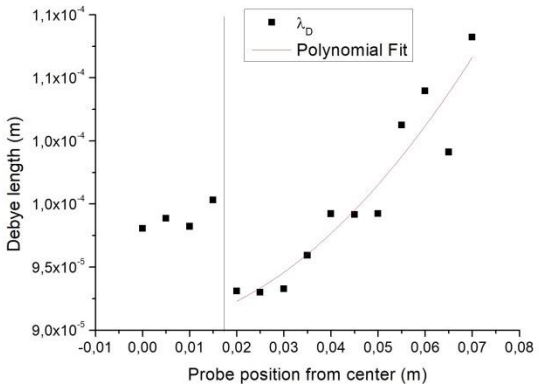

Figure 4: Radial profile of the Debye length measured through the grid electrode. Experimental parameters: p = 1.75 Pa, U_{grid} = 174 V (at 20 W).

Again there is a jump at the position of about 2 cm from the centre, which is mainly due to the discontinuity in the electron density profile. Due to the drop in T_e towards the edge of the IFB the λ_D length increases in vicinity of the grid. This is favourable for the confinement of the IFB, since larger Debye length allows for larger mesh spacing and higher transparency for incoming electrons [3]. The maximum Debye length is more than 110 µm, which indicates that the mesh spacing should be around 220 – 240 microns, which matches the grid constant in the experiments (250 µm) very well.

In addition to the basic plasma parameters inside the IFB, the MRP can also be used to determine the resonance and collision frequency in the plasma. The resonance frequency is usually more than an order of magnitude below the plasma frequency. The resonance frequency remains around 6 x 10^8 Hz throughout most of the plasma. It only drops in the vicinity to the IFB cage down to about 5 x 10^8 Hz due to the slightly lower electron density. The collision frequency in the plasma drops off sharply from 5.5 x 10^8 Hz to 2.5 x 10^8 Hz. towards the edge of the IFB, as shown in Fig. 5 (left).

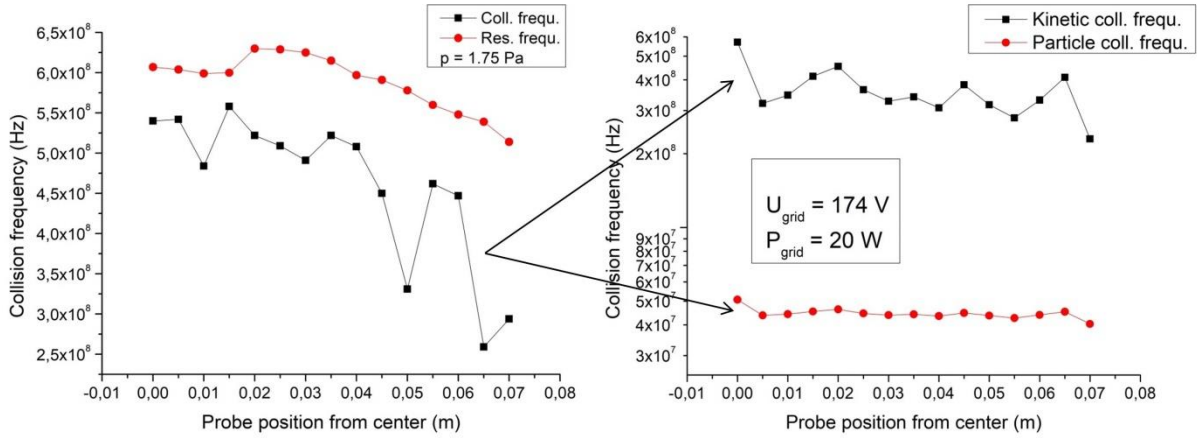

Figure 5: Left: Radial profile of the resonance frequency of the probe (red) and the collision frequency (black) measured through the grid electrode. Right: Contribution of particle collisions (red) and kinetic effects (black) Experimental parameters: p = 1.75 Pa, U_{grid} = 174 V (at 20 W).

The collision frequency in Fig. 5 can be split up into two contributions, which are shown on the right hand side of Fig. 5. The first contribution is the particle collision frequency than includes all physical collisions within the plasma. Since the neutral density is constant throughout the cage electrode, this value remains constant at around 4 x 10^7 Hz. However, there are also so-called kinetic effects. These are basically a measure for the fast electrons that escape from the region of influence of the probe. Thus, these electrons take some of the energy that was coupled into the plasma by the rf-sweep on the probe with them. This fraction of the wave energy is lost for the detection mechanism of the MRP. It is evident from the right hand side of Fig. 5 that at the low pressure of 1.75 Pa more electrons can gain enough energy to escape detection by the probe, while physical particle collisions are comparably rare. Hence, the collision frequency between real particles is about an order of magnitude lower than the effects by escaping electrons.

The next parameter that was investigated was the influence of cage biasing on the plasma parameters. These measurements were done at a constant pressure of 3 Pa at the centre of the IFB. Increasing the bias on the IFB grid anode is expected to increase the plasma density because higher bias voltage produces faster electrons, which can ionise the gas more efficiently. This is firstly due to a larger cross section for ionisation and secondly due to the possibility that some electrons can gain enough kinetic energy to knock out two electrons from a neutral particle or dissociate larger molecules into smaller fragments. The dependence of the electron density is depicted in the following Fig. 6:

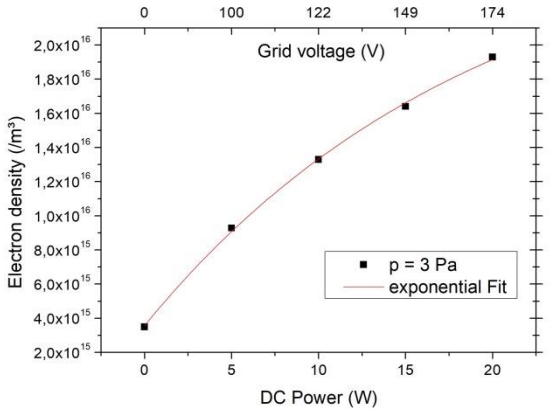

Figure 6: Electron density at 3 Pa as a function of dc power on the grid and grid voltage, respectively.

An increase in grid bias or DC power, respectively, leads to a logarithmic increase of the electron density at the centre of the IFB by roughly an order of magnitude. The logarithmic behaviour stems from the fact that with increasing electron density the Debye length becomes smaller as the electron temperature scales much weaker with grid voltage as is shown in Fig. 7. Even when the electric power on the IFB grid is enhanced four-fold, the electron temperature only increases by some per cent and even decreases slightly at the highest input power. However, this small decrease has to be taken with a grain of salt as the uncertainty of the MRP is 10-15 %, which is quite common for electrical probe diagnostics. There might also be an effect of the complicated chemistry in the Ar/n-hexane plasma that takes place due to excitation, ionisation and dissociation.

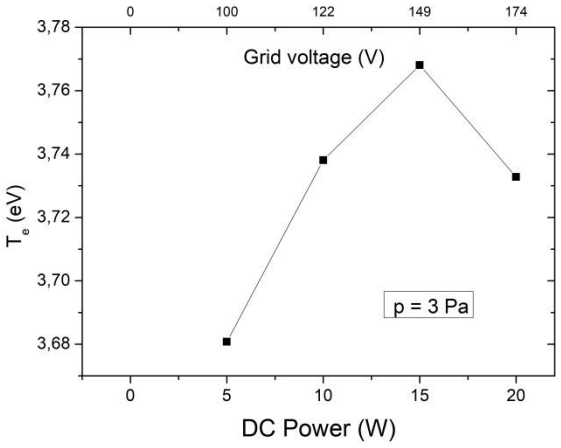

Figure 7: Electron temperature at 3 Pa as a function of dc power on the grid and grid voltage, respectively.

As shown in Fig. 8, λ_D decreases as well, since it is a linear function of electron temperature and density. Again the change in the decrease of the Debye length becomes smaller with higher grid voltage because the confinement at the IFB gets weaker and, thus, the electron density cannot be raised indefinitely.

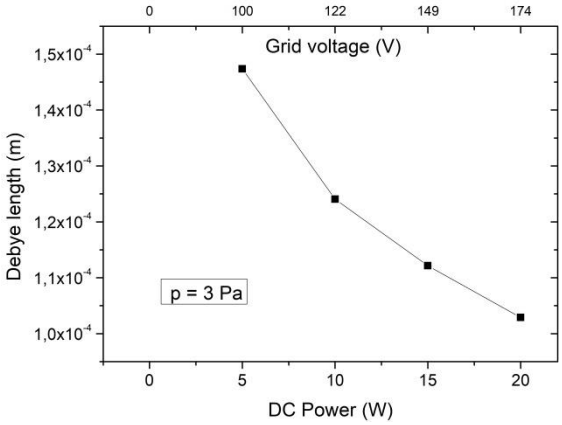

Figure 8: Debye length at 3 Pa as a function of dc power on the grid and grid voltage, respectively.

It may have been noticed that there are no measured data at 0 W dc power on the grid in Figs. 7 and 8. The reason for this is that the background, which exists independently of the IFB, is so thin that the probe data cannot be distinguished from the ground noise. This is also an indication that the onset of an IFB enhances the plasma density considerable, at least within the gridded anode. Such behaviour is also reflected in the collision and resonance frequency, depicted in Fig. 9:

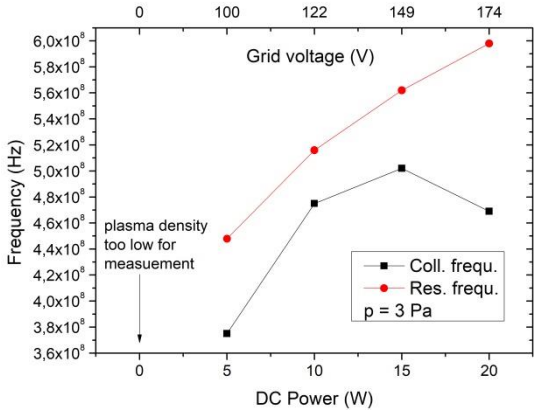

Figure 9: Collision (black) and resonance frequency (red) at 3 Pa as a function of dc power on the grid and grid voltage, respectively.

It can readily be seen in Fig. 9 that the resonance frequency is increasing monotonically with the bias or power on the IFB grid. Although it may seem to increase at the same rate as n_e, it does not. While the electron density increases more than five-fold (from 3.5 x 10^{15} to 1.9 x 10^{16} /m³), the increase in the resonance frequency is about 30 per cent (from 4.5 to 6 x 10^8 Hz). This weaker increase is based on the fact that the resonance frequency of the MRP is close to the plasma frequency, which is only proportional to $(n_e)^{1/2}$. On the other hand, the collision frequency shows a different behaviour: It increases only by about 30 per cent from 3.7 x 10^8 to 5 x 10^8 Hz before it drops off to 4.7 x 10^8 Hz at 20 W dc power on the grid. The drop off at high mesh bias can be explained by the interplay of different factors. In general, the number of collisions between electrons and neutrals tend to increase with increasing bias since faster electrons tend to have larger collision cross sections up to energies of about 50 eV. However, at a pressure of 3 Pa, contributions from physical particle collisions play a minor role, while kinetic effects dominate. This effect becomes even more prominent when the electrons have higher kinetic energy as they can leave the influence volume of the sphere and can be, thus, lost for detection. In addition a mesh at higher bias voltage can absorb more slow electrons that are then not available for physical collisions anymore.

The last set of experiments was conducted with changing pressure, which was increased from 3 to 6 Pa with an intermediate regime at 4 Pa. The voltage on the IFB grid was kept constant at +150 V vs. ground. The results are presented in the following Figs. 10-13:

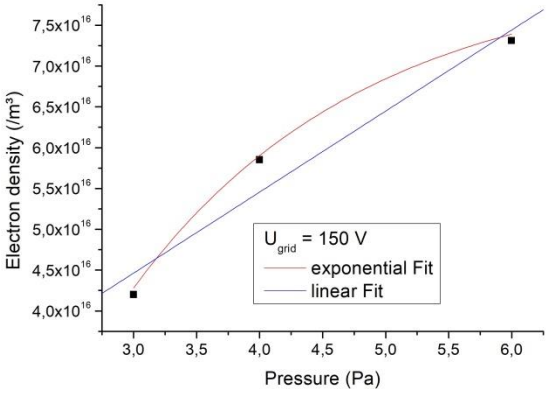

Figure 10: Electron density at U_{grid} = 150 V as a function of increasing pressure.

As before, n_e increases logarithmically with increasing pressure, which is indicated in Fig. 10 by an exponential fit. Since fitting through three points may yield curves that are hard to distinguish (linear, exponential, etc.), both a linear and an exponential fit are shown to prove that the best fit is indeed exponential rather than linear. However, the influence of the pressure increase on the plasma density is weaker than the influence of the grid bias. This is another sign that the IFB setup indeed enhances the charge density in the plasma more significantly than just enhancing the neutral gas pressure. This is explained by a decrease in electron temperature. This decrease stems from the smaller collision mean free path between electrons and neutrals. If the mean energy of the electrons is kept more or less constant, they lose more kinetic energy when creating excited species in inelastic collisions. These excited particles do not contribute to the overall plasma density and slower electrons are less likely to induce further ionisation processes. The decrease in T_e is also experimentally verified and presented in Fig. 11:

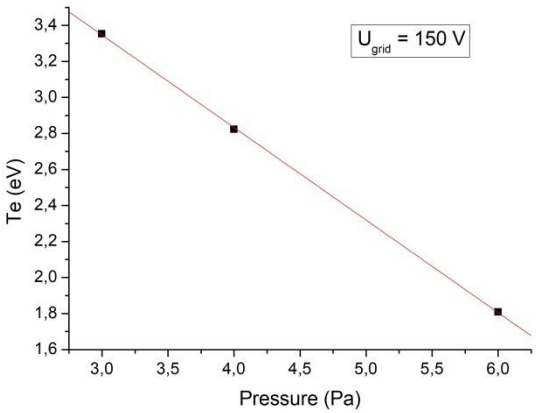

Figure 11: Electron temperature at U_{grid} = 150 V as a function of increasing pressure.

Here it is obvious that the decline in electron temperature scales linearly with increasing pressure. The combination of diminished electron temperature und increasing density is also reflected in a significant reduction of the Debye length as shown in Fig. 12:

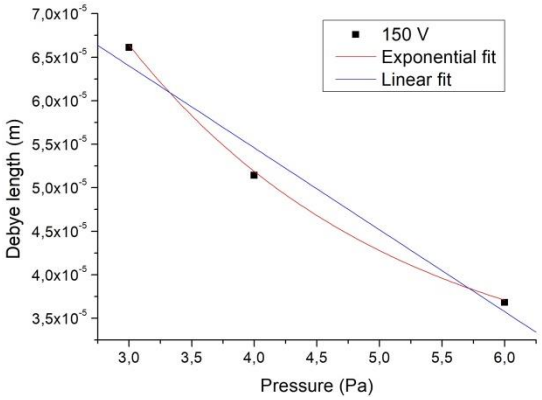

Figure 12: Debye length at U_{grid} = 150 V as a function of increasing pressure.

λ_D is reduced by more than 50 per cent in the centre of the IFB. The Debye length will decrease to some extend with increasing pressure. Thus, the working gas pressure in the plasma chamber in combination with the grid constant of the IFB mesh sets a natural limit for the application of IFBs. This has to be taken into account when choosing the grid for the IFB anode. A final look on the data for the collision and resonance frequency is depicted in Fig. 13:

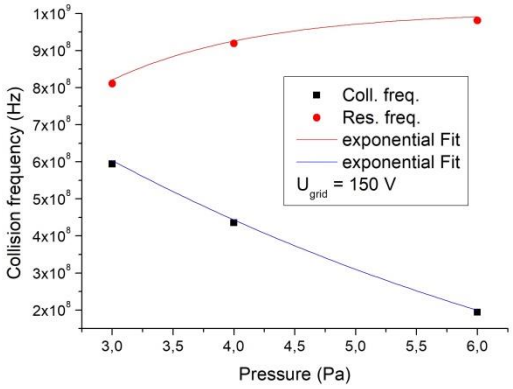

Figure 13: Collision frequency (red) and resonance frequency (black) at U_{grid} = 150 V as a function of increasing pressure.

While the resonance frequency is increasing to nearly 1 GHz, the collision frequency is decreasing significantly. The latter, counter intuitive behaviour can again be explained by the collision mean free path, which is still rather large. Hence, the particles can escape the relevant volume before they are detected by the probe.

IV. Conclusion

In this work measurements of the basic plasma parameters in a reactive Ar/n-hexane IFB were measured for the first time with an MRP. It was shown that the plasma density within the IFB can be increased significantly by increasing the bias on the grid electrode. This effect is much stronger than increasing the pressure at constant grid voltage. Additionally, it can be concluded from the measured data that the increase in plasma density can be achieved very efficient as the energy input on the IFB mesh increased by less than 50 per cent while the charge density increased by more than an order of magnitude. Furthermore, the measurements showed that the MRP is well suited for experiments in chemically reactive plasma. The only drawback was found to be the fact that under certain circumstances the determination of the collision frequency within the plasma might be influenced or even dominated by kinetic effects. This is in particular an issue when the kinetic particle energy is high and the pressure is low. The conducted experiments also showed that the understanding of the chemical processes within an IFB must still be improved, which is beyond the scope of this work. However, this will be left for future work. It was also demonstrated that increasing the grid bias of the IFB anode enhances the collision frequency, partly because the overall cross section of electron-neutral collisions becomes larger with higher kinetic energies of the negative charge carriers. This effect is somewhat countered by electrons with very high kinetic energy that move too quickly too far away from the probe and, hence, cannot contribute to the measured collision frequencies. This mechanism is even more pronounced in the low pressure regime in which these experiments were conducted. Even at 6 Pa the contribution of kinetic effects to the measured collision frequencies is low enough that seemingly the overall collision frequency shrinks with increasing pressure. Also this is a point that should be taken into account when evaluation MRP data in low pressure plasma. In the future the use of an MRP for IFB experiments will be continued in order to gain even more insights into the physical properties of IFBs in reactive plasma. It is also planned to investigate other parameters such as the electron energy distribution function, the plasma potential, etc. However, this will include the usage of several additional diagnostic techniques, such as Langmuir probes, retarding field analysers and optical diagnostics.

V. Acknowledgements

This work was partly funded by the German Federal Ministry for Economic Affairs and Climate Action and the European Social Fund as project House of Plasma (03EFRNW279) in the EXIST program.

VI. References

[1] R. L. Stenzel, et al. "Transit time instabilities in an inverted fireball. I. Basic properties." *Phys. Plasmas* 18.1, 012104, 2011. https://doi.org/10.1063/1.3533437

[2] R. L. Stenzel, et al. "Transit time instabilities in an inverted fireball. II. Mode jumping and nonlinearities." *Phys. Plasmas* 18.1, 012105, 2011. https://doi.org/10.1063/1.3533440

[3] J. Gruenwald, J. Reynvaan, and P. Knoll. "Creation and characterization of inverted fireballs in H_2 plasma." *Phys. Scr.* 2014.T161 014006, 2014. https://doi.org/10.1088/0031-8949/2014/T161/014006

[4] J. Gruenwald, "On the dispersion relation of the transit time instability in inverted fireballs." *Phys. Plasmas* 21.8 082109, 2014. https://doi.org/10.1063/1.4892555

[5] D. Levko, and J. Gruenwald. "On the energy deposition into the plasma for an inverted fireball geometry." *Phys. Plasmas* 24.10 103519, 2017. https://doi.org/10.1063/1.4998548

[6] V. Mitra, et al. "Mixed mode oscillations in presence of inverted fireball in an excitable DC glow discharge magnetized plasma." *Phys. Plasmas* 24.2 022307, 2017. https://doi.org/10.1063/1.4976320

[7] J. Gruenwald, J. Reynvaan and P. Geistlinger. "Basic plasma parameters and physical properties of inverted He fireballs." *Plasma Sources Sci. Technol.* 27.1 (2018): 015008. https://doi.org/10.1088/1361-6595/aaa332

[8] J. Gruenwald, J. Reynvaan and P. Geistlinger. "Influence of inhomogeneous electrode biasing on the plasma parameters of inverted H2 fireballs." *J. Technol. Space Plasmas* 1.1 (2020): 1-4. https://doi.org/10.31281/2018/000002

[9] J. Gruenwald, and C. Teodorescu. "On the dispersion relation for the Buneman instability in spherically confined plasmas." *Plasma Phys. Contr. F.* 61.3 (2019): 035007. https://doi.org/10.1088/1361-6587/aaf949

[10] J. Reynvaan, et al. "Multiple Fireballs in a Reactive H_2/CH_4 Plasma." *IEEE Trans. Plasma Sci.* 42.10 (2014): 2848-2849. https://doi.org/10.1109/TPS.2014.2301494

[11] P. Knoll, et al. "PECVD of carbon by inverted fireballs: From sputtering, bias enhanced nucleation to deposition." *Diam. Relat. Mater.*65 (2016): 96-104. https://doi.org/10.1016/j.diamond.2016.02.021Get

[12] M. Mayer, et al. "Diamond like carbon deposition by inverted fireballs." *Mater. Today: Proc.* 3 (2016): S184-S189. https://doi.org/10.1016/j.matpr.2016.02.031

[13] J. Gruenwald, et al. "Application and limitations of inverted fireballs in a magnetron sputter device." *Surf. Coat. Technol.* 422 (2021): 127510. https://doi.org/10.1016/j.surfcoat.2021.127510

[14] M. Lapke, T. Mussenbrock, and R. P. Brinkmann. "The multipole resonance probe: A concept for simultaneous determination of plasma density, electron temperature, and collision rate in low-pressure plasmas." *Appl. Phys. Lett.* 93 051502, 2008. http://dx.doi.org/10.1063/1.2966351

[15] M. Lapke, J. Oberrath, C. Schulz, R. Storch, T. Styrnoll, C. Zietz, P. Awakowicz, R. P. Brinkmann, T. Musch, and T. Mussenbrock. "The multipole resonance probe: characterization of a prototype." *Plasma Sources Sci. Technol.* 20 042001, 2011. http://dx.doi.org/10.1088/0963-0252/20/4/042001

[16] C. Schulz, T. Styrnoll, R. Storch, P. Awakowicz, T. Musch, and I. Rolfes. "The Multipole Resonance Probe: Progression and Evaluation of a Process Compatible Plasma Sensor." *IEEE Sensors J.* 14 3408-3417, 2014. http://dx.doi.org/10.1109/JSEN.2014.2333659

[17] T. Styrnoll. "Die Multipolresonanzsonde: Vom Demonstrator zur industrietauglichen Plasmadiagnostik." PhD Thesis, Ruhr University Bochum, 2015

[18] D. Pohle, C. Schulz, M. Oberberg, A. Serwa, P. Uhlig, P. Awakowicz, and I. Rolfes. "Progression of the Multipole Resonance Probe: Advanced Plasma Sensors Based on LTCC-Technology." *48th European Microwave*

Conference (EuMC) 239-242, 2018 https://doi.org/10.23919/EuMC.2018.8541730

[19] M. Fiebrandt, M. Oberberg, and P. Awakowicz. "Comparison of Langmuir probe and multipole resonance probe measurements in argon, hydrogen, nitrogen, and oxygen mixtures in a double ICP discharge." *J. Appl. Phys.* 122.1 013302, 2017. https://doi.org/10.1063/1.4991493

[20] J. Zheng, Y. Tao and D. G. Truhlar. "Multi-structural thermodynamics of C–H bond dissociation in hexane and isohexane yielding seven isomeric hexyl radicals." *Phys. Chem. Chem. Phys.* 13.43 (2011): 19318-19324. https://doi.org/10.1039/C1CP21829H

[21] R. G. Pierce, G. Padron-Wells, and M. J. Goeckner. "Gas-phase chemistry of pulsed n-hexane discharge." *Plasma Chem. Plasma Process.* 29.1 (2009): 1-11. https://doi.org/10.1007/s11090-008-9157-8

[22] E. Szymańska, et al. "Dissociative electron attachment to acetaldehyde, CH 3 CHO. A laboratory study using the velocity map imaging technique." *Phys. Chem. Chem. Phys.* 15.3 (2013): 998-1005. https://doi.org/10.1039/C2CP42966G

[23] O. Sueoka, et al. "Total cross-section measurements for positrons and electrons colliding with alkane molecules: Normal hexane and cyclohexane." *Phys. Rev. A* 72.4 (2005): 042705. https://doi.org/10.1103/PhysRevA.72.042705